Supplementary Information

Structure and dynamics of the interaction of Delta and Omicron BA.1 SARS-CoV-2 variants with REGN10987 Fab reveal mechanism of antibody action

Ekaterina N. Lyukmanova[1,2,3,6,#], Evgeny B. Pichkur[4,6], Dmitry E. Nolde[2,6], Milita V. Kocharovskaya[2], Valentin A. Manuvera[5], Dmitriy A. Shirokov[5], Daria D. Kharlampieva[5], Ekaterina N. Grafskaia[5], Julia I. Svetlova[5], Vassili N. Lazarev[5], Anna M. Varizhuk[5], Mikhail P. Kirpichnikov[1,2,3], Zakhar O. Shenkarev[2,#]

1 Department of Biology, MSU-BIT Shenzhen University, 518172 Shenzhen, China
2 Shemyakin-Ovchinnikov Institute of Bioorganic Chemistry, Russian Academy of Sciences, 119997 Moscow, Russia
3 Interdisciplinary Scientific and Educational School of Moscow University “Molecular Technologies of the Living Systems and Synthetic Biology”, Faculty of Biology, Lomonosov Moscow State University, 119234 Moscow, Russia
4 Department of Molecular and Radiation Biophysics, Petersburg Nuclear Physics Institute named by B.P.Konstantinov of National Research Center "Kurchatov Institute", 188300 Gatchina, Russia
5 Lopukhin Federal Research and Clinical Center of Physical-Chemical Medicine of Federal Medical Biological Agency, 119435 Moscow, Russia
6 These authors contributed equally: Ekaterina N. Lyukmanova, Evgeny B. Pichkur, Dmitry E. Nolde.

#Correspondence:
Ekaterina N. Lyukmanova, lyukmanova_ekaterina@smbu.edu.cn;
Zakhar O. Shenkarev, zakhar-shenkarev@yandex.ru

Analysis of replica convergence

Calculated correlation coefficients (R) between the sets of the lifetimes of 62 possible intermolecular contacts for each MD trajectory revealed the difference in convergence of replicas for the different RBD variants (Supplementary Data 1-9 and 1-10). Good reproducibility was observed for the Wuhan, Omicron, N501Y, and 'Others' MD trajectories (minimal correlation coefficient between the three replicas for each of these RBD variants $R_{MIN} > 0.3$, $p < 0.02$, n = 62 intermolecular contacts), while N440K, G446S, and Q498R demonstrated weak inter-replica correlation ($R_{MIN} < 0.3$). Comparison of the individual replicas revealed that the Wuhan, N440K, G446S, Q498R, N501Y, and 'Others' trajectories form a group with high similarity (maximal correlation coefficient between replicas for each pair of these RBD variants $R_{MAX} > 0.5$, $p < 4\times10^{-5}$, n = 62), while the Omicron MD replicas were dissimilar to MD trajectories of all other RBD variants except N440K ($R_{MAX} < 0.5$).

Supplementary Tables

Supplementary Table 1. Amino-acid sequences of Fab fragment of the REGN10987 antibody and its recombinant analogue.

REGN10987 Fab fragment heavy chain
QVQLVESGGGVVQPGRSLRLSCAASGFTFSNYAMYWVRQAPGKGLEWVAVISYDGSNKYYADSVKGRFTISRD NSKNTLYLQMNSLRTEDTAVYYCASGSDYGDYLLVYWGQGTLVTVSSASTKGPSVFPLAPSSKSTSGGTAALG CLVKDYFPEPVTVSWNSGALTSGVHTFPAVLQSSGLYSLSSVVTVPSSSLGTQTYICNVNHKPSNTKVDKKVE PKSCDK

Recombinant analogue Fab fragment heavy chain
QVQLVESGGGVVQPGRSLRLSCAASGFTFSNYAMYWVRQAPGKGLEWVAVISYDGSNKYYADSVKGRFTISRD NSKNTLYLQMNSLRTEDTAVYYCASGSDYGDYLLVYWGQGTLVTVSSASTKGPSVFPLAPSSKSTSGGTAALG CLVKDYFPEPVTVSWNSGALTSGVHTFPAVLQSSGLYSLSSVVTVPSSSLGTQTYICNVNHKPSNTKVDKKVE PKSCDK

REGN10987 Fab fragment light chain
QSALTQPASVSGSPGQSITISCTGTSSDVGGYNYVSWYQQHPGKAPKLMIYDVSKRPSGVSNRFSGSKSGNTA SLTISGLQSEDEADYYCNSLTSISTWVFGGGTKLTVLGQPKAAPSVTLFPPSSEELQANKATLVCLISDFYPG AVTVAWKADSSPVKAGVETTTPSKQSNNKYAASSYLSLTPEQWKSHRSYSCQVTHEGSTVEKTVAPTECS

Recombinant analogue Fab fragment light chain
QSALTQPASVSGSPGQSITISCTGTSSDVGGYNYVSWYQQHPGKAPKLMIYDVSKRPSGVSNRFSGSKSGNTA SLTISGLQSEDEADYYCNSLTSISTWVFGGGTKLTVLGRTVAAPSVFIFPPSDEQLKSGTASVVCLLNNFYPR EAKVQWKVDNALQSGNSQESVTEQDSKDSTYSLSSTLTLSKADYEKHKVYACEVTHQGLSSPVTKSFNRGEC

Differences are shown by color.

Supplementary Table 2. Oligonucleotides used for mutagenesis and cloning of the RBD variants.

Oligonucleotide name	5'→3' sequence
KramRBD-F	cta<u>tctaga</u>gcctctgctaaccatg
KramRBD-R	ata<u>ctcgag</u>tcgcgacttaagatcg
L452R-For	tacaattac**cgg**taccggctgttccggaag
L452R-Rev	acagccggta**ccg**gtaattgtagttgccgccg
T478K-For	gccggcagc**aag**ccttgtaacggcgtggaag
T478K-Rev	cgttacaagg**ctt**gctgccggcctgatagatc
N440K-For	gaacagcaacaa**g**ctggactccaaagtcggcg
N440K-Rev	ttggagtccag**c**ttgttgctgttccaggcaatc
G446S-For	actccaaagtc**a**gcggcaactacaattaccg
G446S-Rev	gtagttgccgc**t**gactttggagtccaggttg
Q498R-For	tacggctttc**g**gcccacaaatggcgtgggc
Q498R-Rev	atttgtgggc**c**gaaagccgtaggactgcag
N501Y-For	ctttcagcccaca**t**atggcgtgggctatcagcc
N501Y-Rev	gcccacgccat**a**tgtgggctgaaagccgtag
G339D-For	gtgcccttcg**a**cgaggtgttcaatg
G339D-Rev	cattgaacacctcg**t**cgaaggggcac
371-373-375-F	gtacaact**tg**gcc**cc**cttc**tt**caccttcaag
371-373-375-R	cttgaaggtg**aa**gaag**gg**ggc**ca**agttgtac
K417N-For	ctggacagacaggcaa**c**atcgccgactacaac
K417N-Rev	gttgtagtcggcgat**g**ttgcctgtctgtccag
440-446-For	gaacagcaacaa**g**ctggactccaaagtc**a**gcggcaactac
440-446-Rev	gtagttgccgc**t**gactttggagtccag**c**ttgttgctgttc
477-478-484-F	ctatcaggccggca**a**ca**ag**ccttgtaacggcgtgg**c**aggcttcaac
477-478-484-R	gttgaagcct**g**ccacgccgttacaagg**ct**tg**t**tgccggcctgatag
484-493-Rev	**t**gtaggac**cg**cagtgggaagtagcagttgaagcct**g**ccac
493-496-498-501-505-R	at**g**ggcccacgccat**a**tgtgggc**c**gaaagc**t**gtaggac**cg**cagtgggaag
501-505-For	ccaca**t**atggcgtgggc**c**atcagccctacagagtggtggtg

Restriction sites *Xba*I and *Xho*I are underlined, mutations are highlighted in bold.

Supplementary Figures

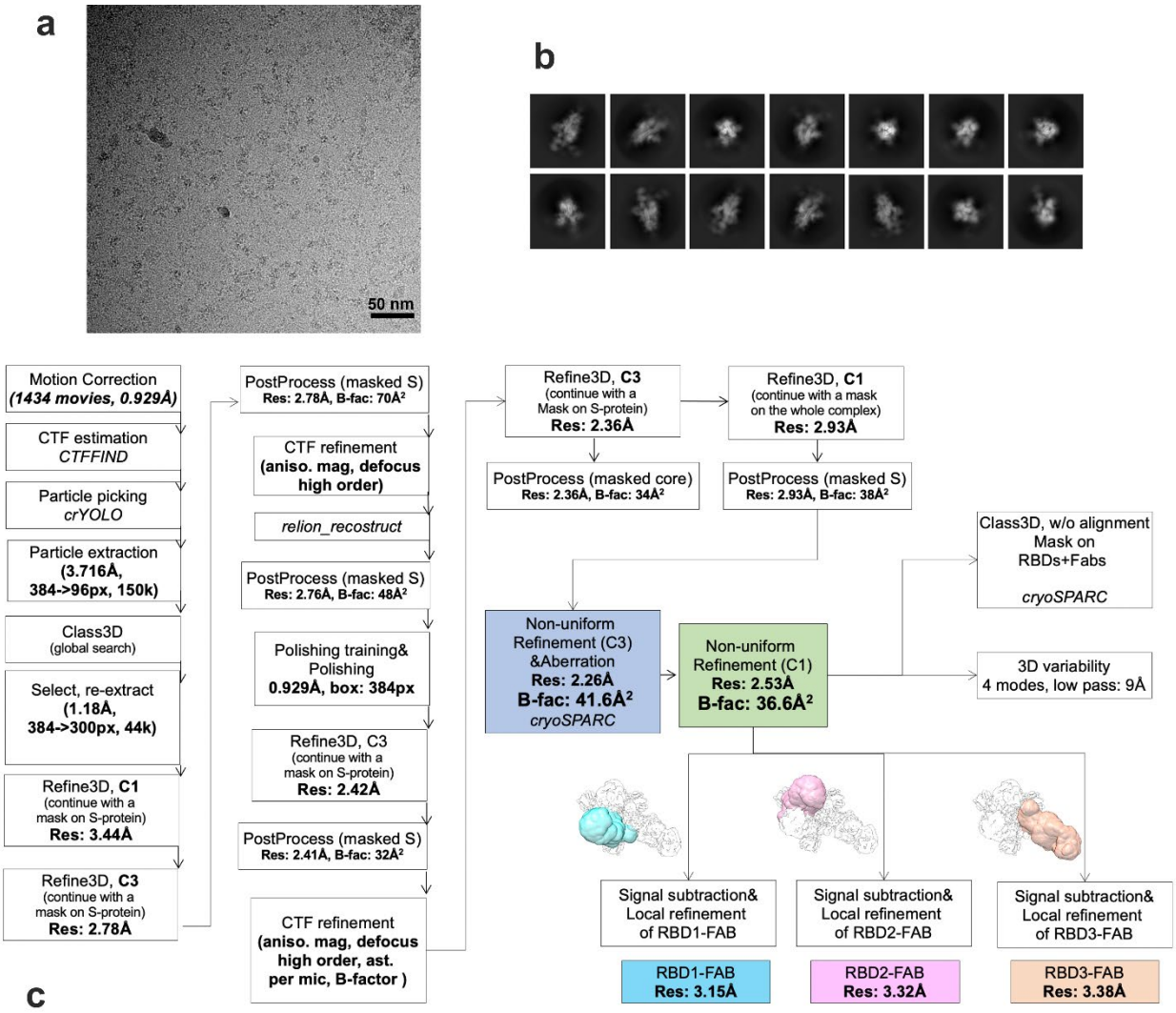

Supplementary Figure 1. Cryo-EM data processing of the Delta S-protein in complex with REGN10987-Fab. a Representative cryo-EM image, scale bar is 50 nm. **b** 2D classes. **c** Workflow of the data processing.

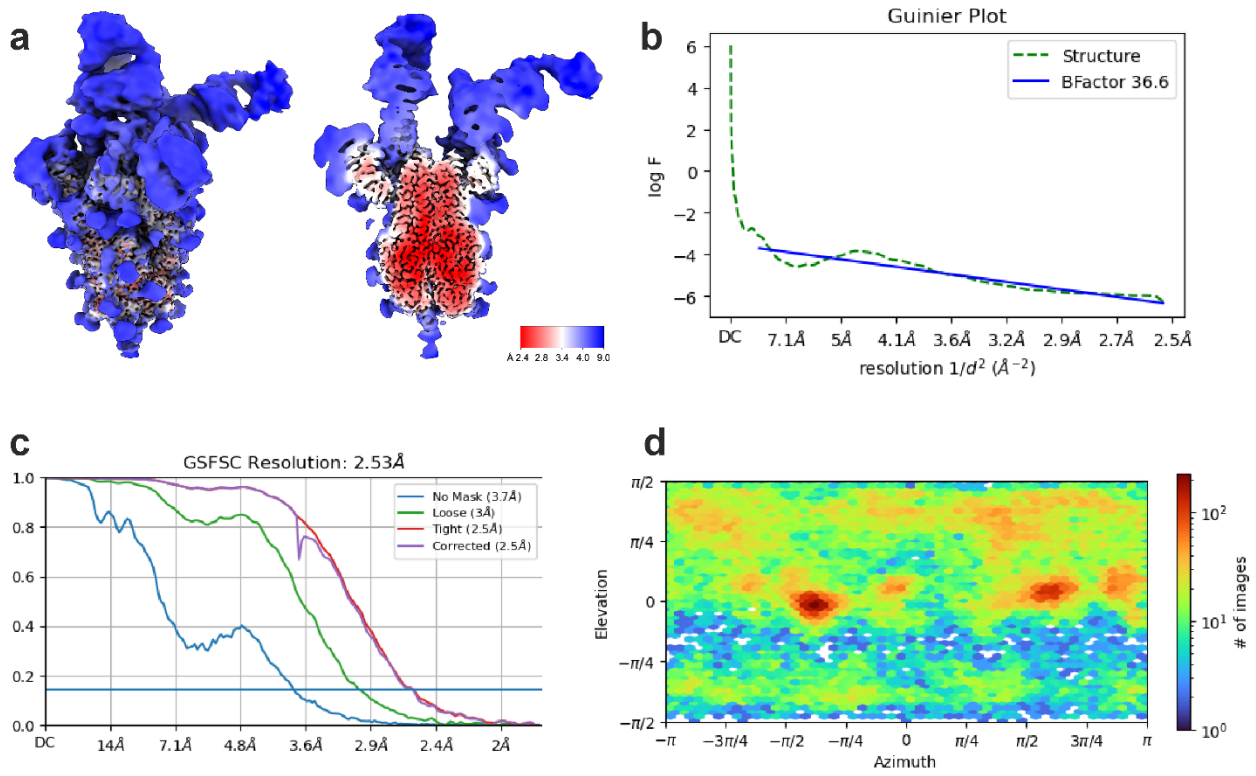

Supplementary Figure 2. Quality assessment of the cryo-EM structure determined for Delta S-protein in complex with REGN10987-Fab. a Local resolution map of the full structure. **b** Fourier shell correlation (FSC=0.143). **c** Guinier plot for corresponding structure. **d.** Particles distribution map calculated in cryoSPARC.

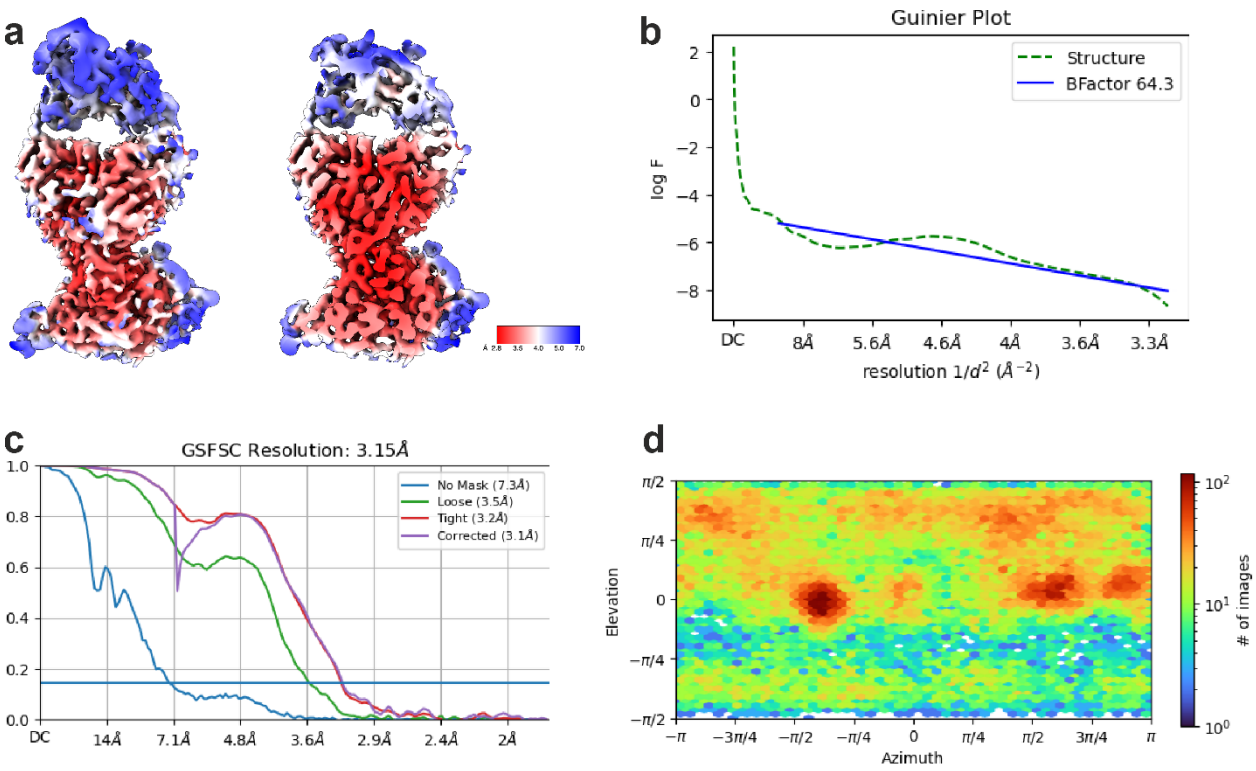

Supplementary Figure 3. Quality assessment of the cryo-EM structure determined for Delta S-protein in complex with REGN10987-Fab after local refinement of the RBD1/Fab1 region. a Local resolution map of the RBD1/Fab1 structure. **b** Fourier shell correlation plot (FSC=0.143) for RBD1/Fab1 structure. **c** Guinier plot for corresponding structure. **d.** Particles distribution map calculated in cryoSPARC.

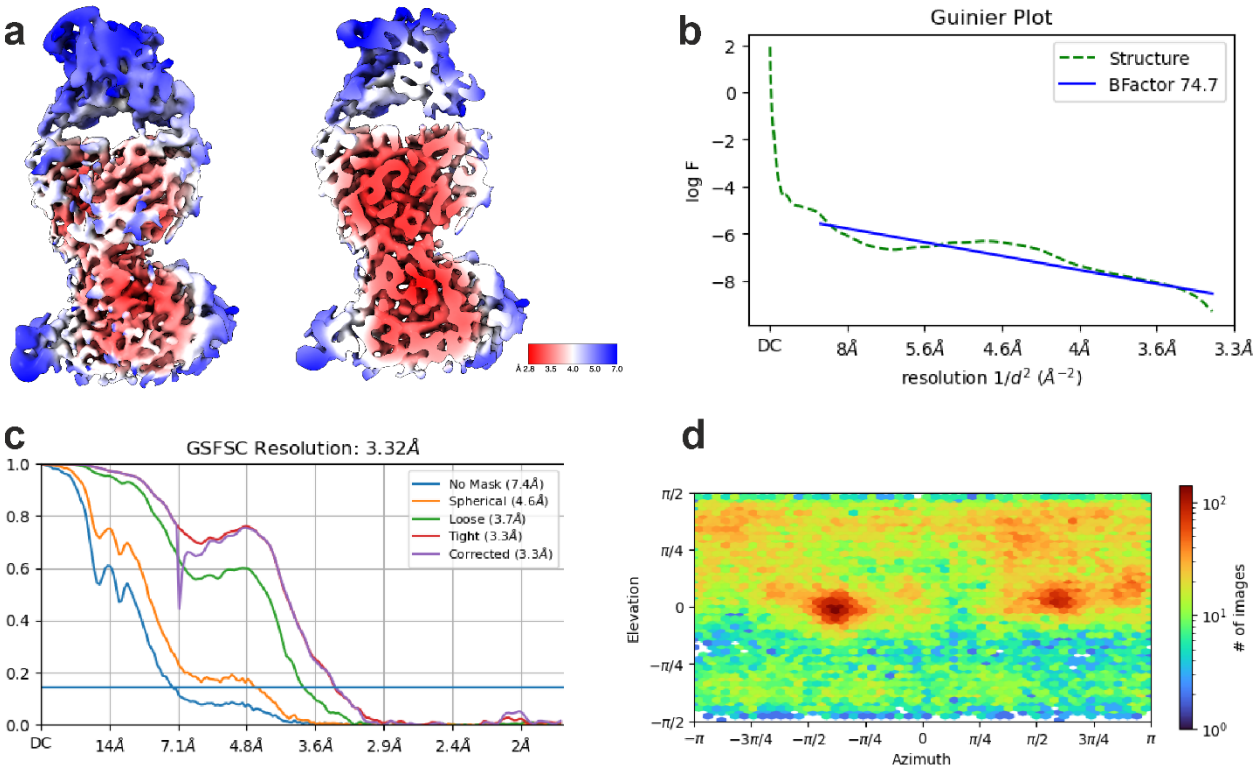

Supplementary Figure 4. Quality assessment of the cryo-EM structure determined for Delta S-protein in complex with REGN10987-Fab after local refinement of the RBD2/Fab2 region. a Local resolution map of the RBD2/Fab2 structure. **b** Fourier shell correlation plot (FSC=0.143) for RBD2/Fab2 structure. **c** Guinier plot for corresponding structure. **d.** Particles distribution map calculated in cryoSPARC.

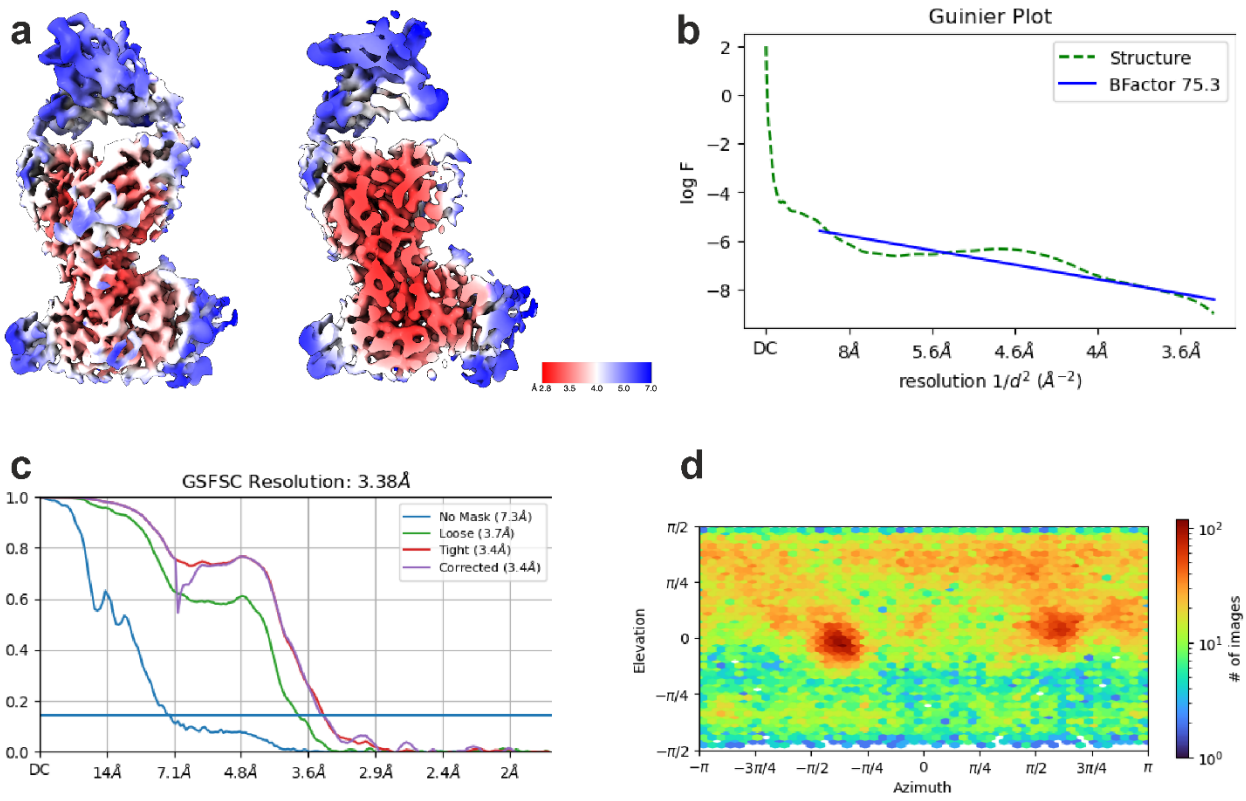

Supplementary Figure 5. Quality assessment of the cryo-EM structure determined for Delta S-protein in complex with REGN10987-Fab after local refinement of the RBD3/Fab3 region. a Local resolution map of the RBD3/Fab3 structure. **b** Fourier shell correlation plot (FSC=0.143) for RBD3/Fab3 structure. **c** Guinier plot for corresponding structure. **d.** Particles distribution map calculated in cryoSPARC.

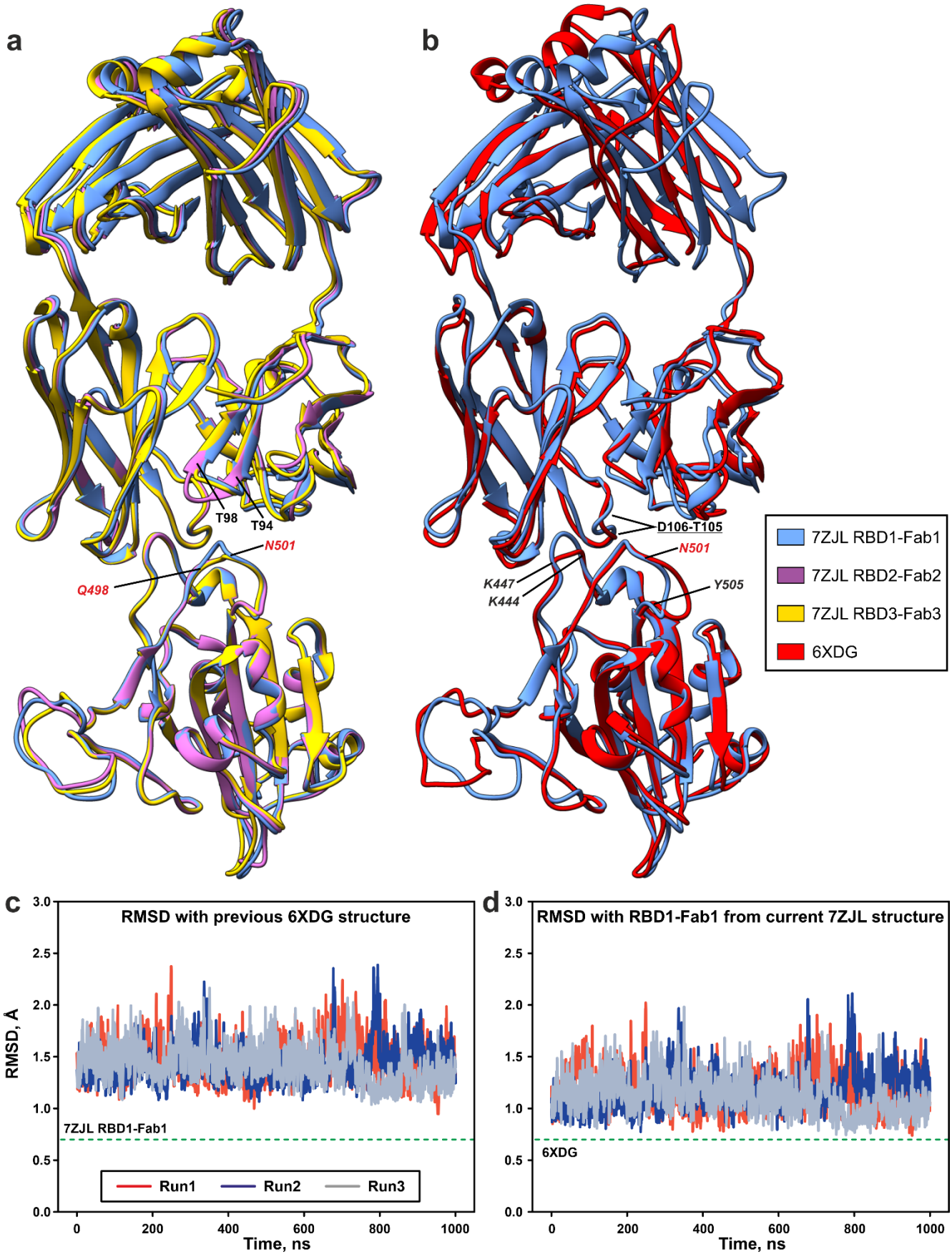

Supplementary Figure 6. Overlay of the RBD/REGN10987-Fab structures determined by cryo-EM. (a) Superposition of the three RBD/Fab structures from the Delta S-protein/REGN10987-Fab complex obtained by local refinement (PDB 7ZJL, present work). **(b)** Superposition of the obtained here

Delta-RBD1/REGN10987-Fab1 structure with the published structure of WT-RBD/REGN10987-Fab (PDB 6XDG [1]). **(c,d)** Comparison of the RBD-Fab interfaces in the previously published 6XDG structure (**c**) and the 7ZJL structure presented here (**d**) with MD trajectories of the WT-RBD/REGN10987-Fab complex (three replicas, Run1 to Run3). The structures were superimposed on the β-structural regions of the RBD (354-358, 375-380, 393-403, 431-437, 507-516). RMSD values between coordinates of CA atoms from the N437-N450 and Q498-Y508 RBD loops were calculated. MD data are overaged over 5 ns window. RMSD in this RBD region between the presented here and previous structures is ~ 0.7 Å (dashed lines, panels **c,d**).

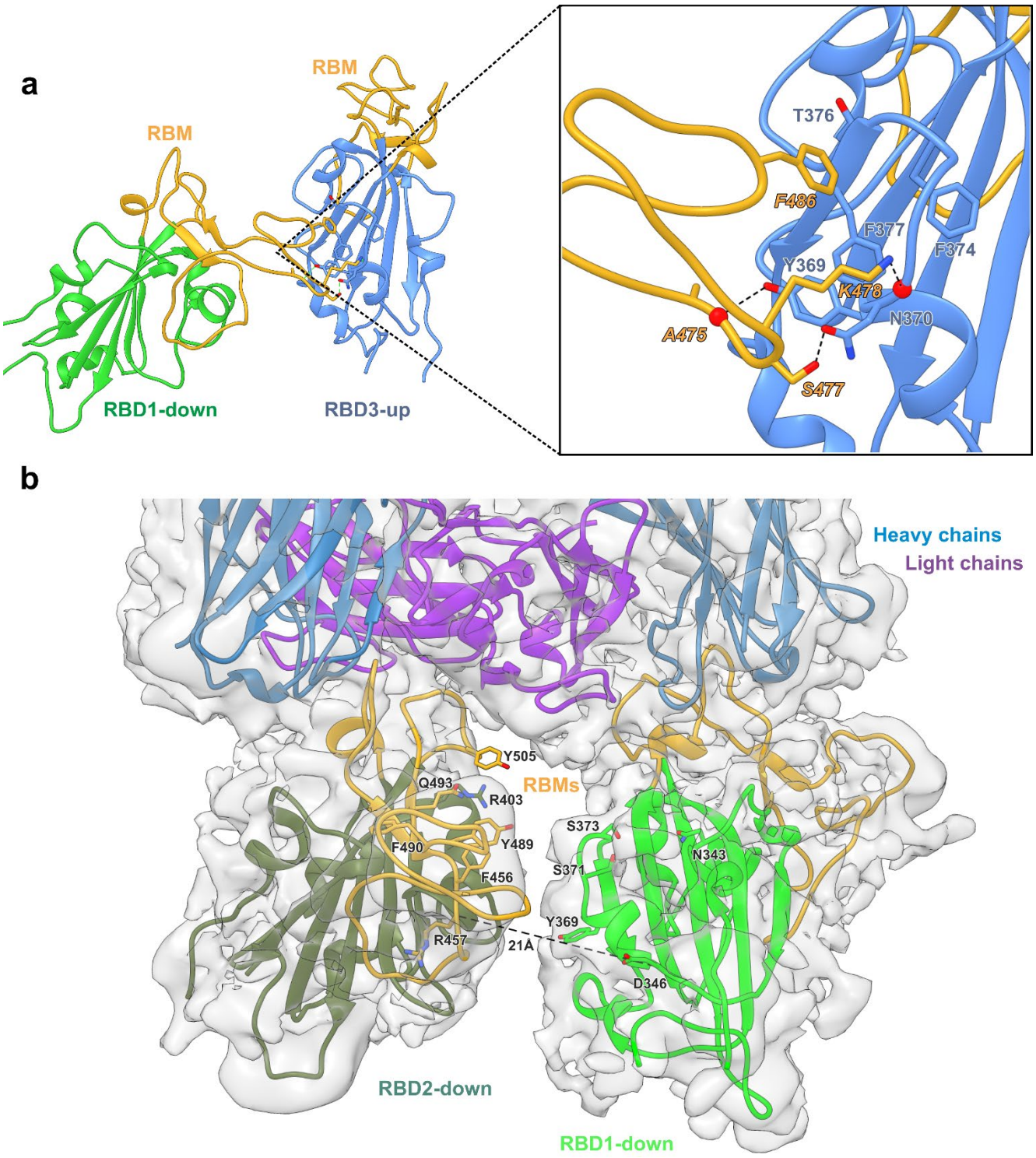

Supplementary Figure 7. RBD-RBD interactions in the Delta S-protein/REGN10987-Fab complex. (a) Interactions between RBD1-down and RBD3-up in the overall structure of the complex. Backbone CO-groups are shown as red spheres. (**b**) Structure of the RBD1-down/Fab1+RBD2-down/Fab2 region determined by local refinement with resolution of 3.8 Å. The distance between CA of D346-RBD1 and R457-RBD2 is shown.

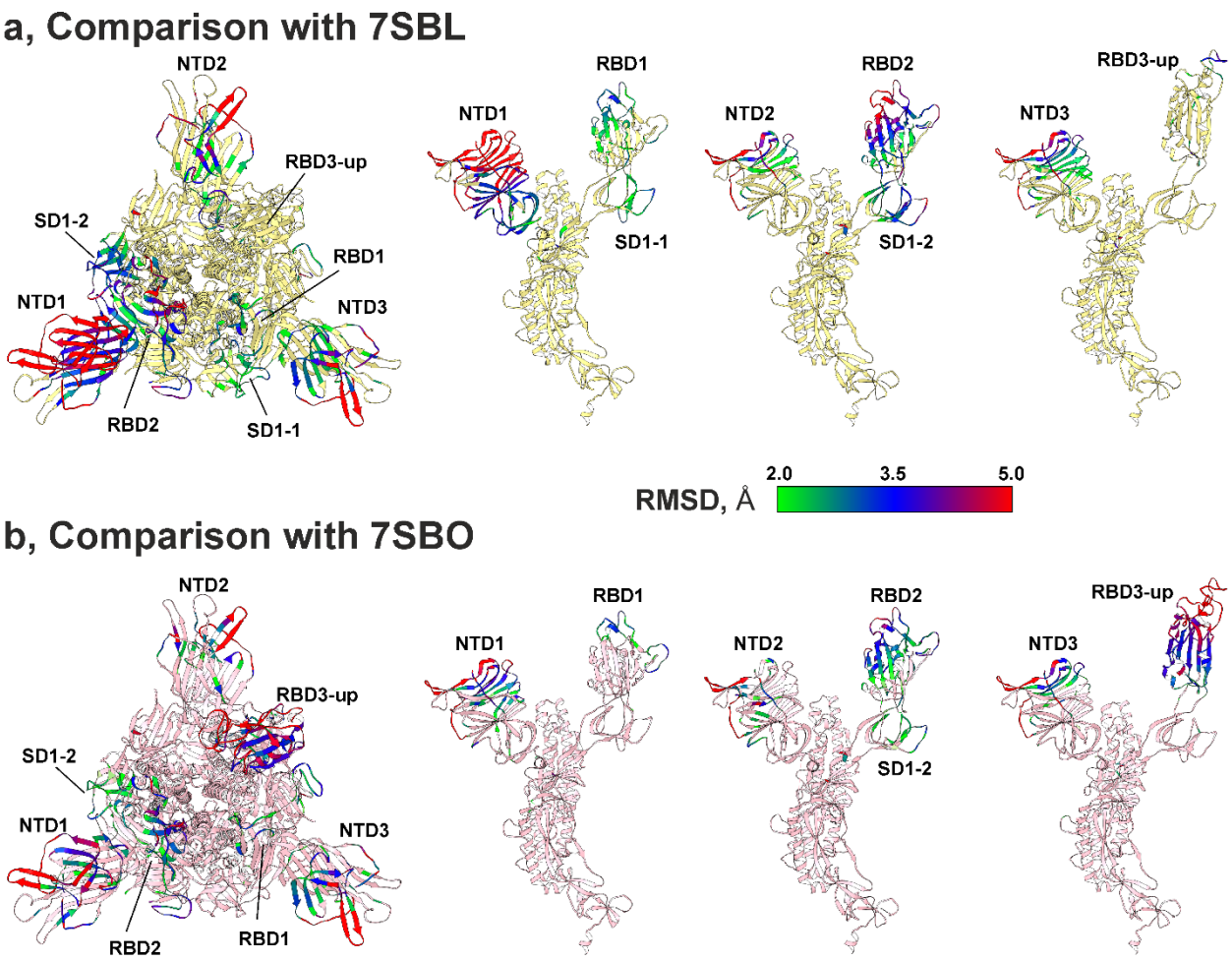

Supplementary Figure 8. Comparison of the Delta S-protein structure in the complex with REGN10987-Fab (present work) with the published structures of *apo* Delta S-protein in the one-RBD-up conformation (PDB 7SBL and 7SBO [2]). Top-view of the trimeric S-protein (without Fab) and side-views of individual protomers are shown. Backbone of the S-protein is colored according to local RMSD between the structures (see legend).

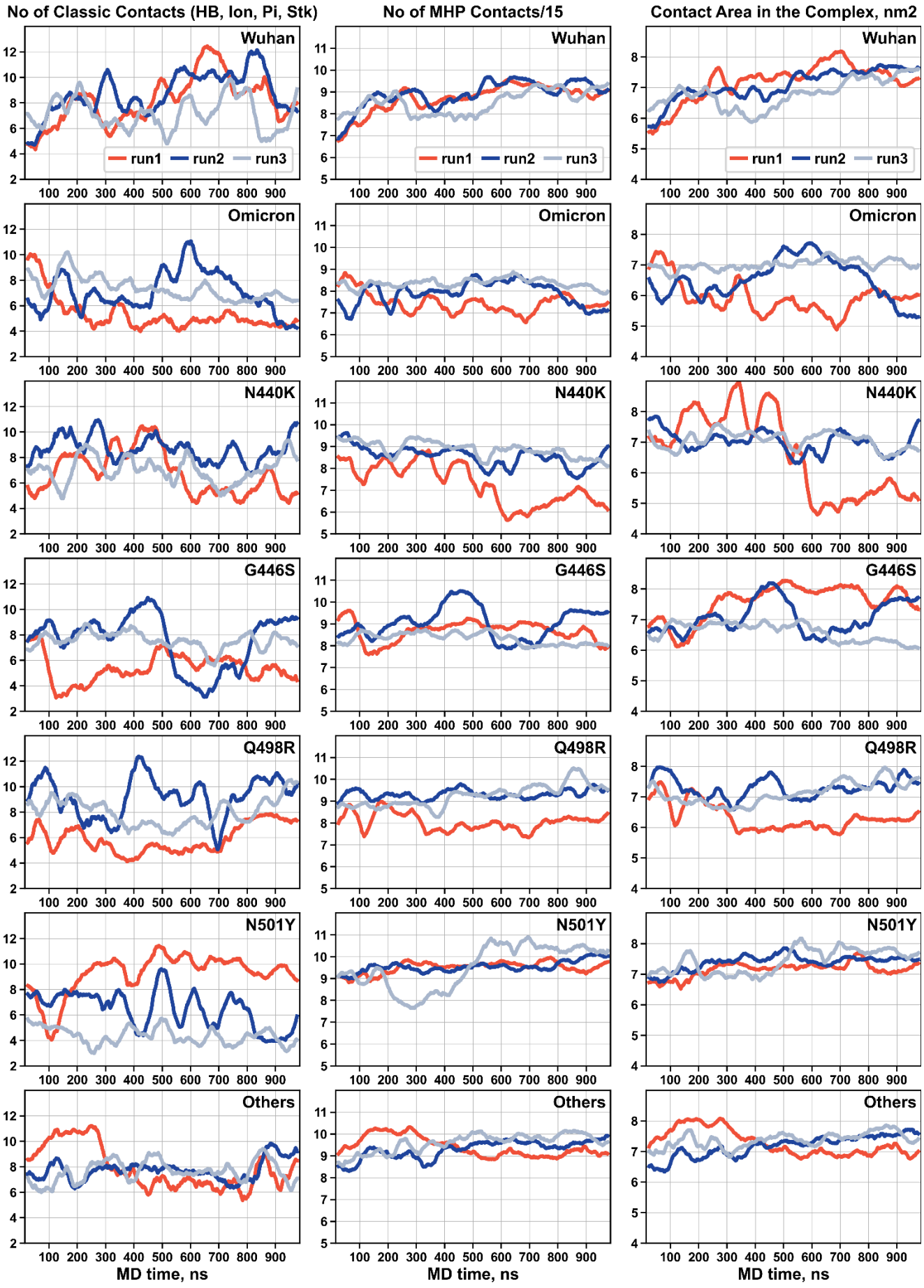
No of Classic Contacts (HB, Ion, Pi, Stk)
No of MHP Contacts/15
Contact Area in the Complex, nm2
Wuhan
Omicron
N440K
G446S
Q498R
N501Y
Others
run1
run2
run3
MD time, ns

Supplementary Figure 9. Characteristics of 1 μs MD trajectories of the RBD/REGN10987-Fab complexes. The following RBD variants were modelled: Wuhan (WT), Omicron BA.1, Delta/N440K, Delta/G446S, Delta/Q498R, Delta/N501Y, and 'Others' (Delta RBD containing 10 remaining Omicron BA.1 mutations: G339D, S371L, S373P, S375F, K417N, S477N, E484A, Q493R, G496S, Y505H). Note that Delta RBD differs from Wuhan RBD by two mutations (T478K and L452R) located away from the REGN10987 binding site. One of these mutations (T478K) is common for the Delta and Omicron variants (Fig. 1e). Three MD replica were calculated for each complex (run1, run2, run3). (Left column) Total number of the 'classic' RBD-Fab interactions (ionic, hydrogen bonds, π-cation, and stacking) at each timepoint of the MD trajectory. (Middle column) Total number of the molecular hydrophobicity potential (MHP) contacts divided by 15. The scaling factor '15' was used to approximately equalize the number of 'classic' and MHP contacts. MHP contacts include hydrophobic-hydrophobic and polar-polar intermolecular interactions. (Right column) RBD-Fab contact area in the complex (nm^2). All data are overaged over 50 ns window.

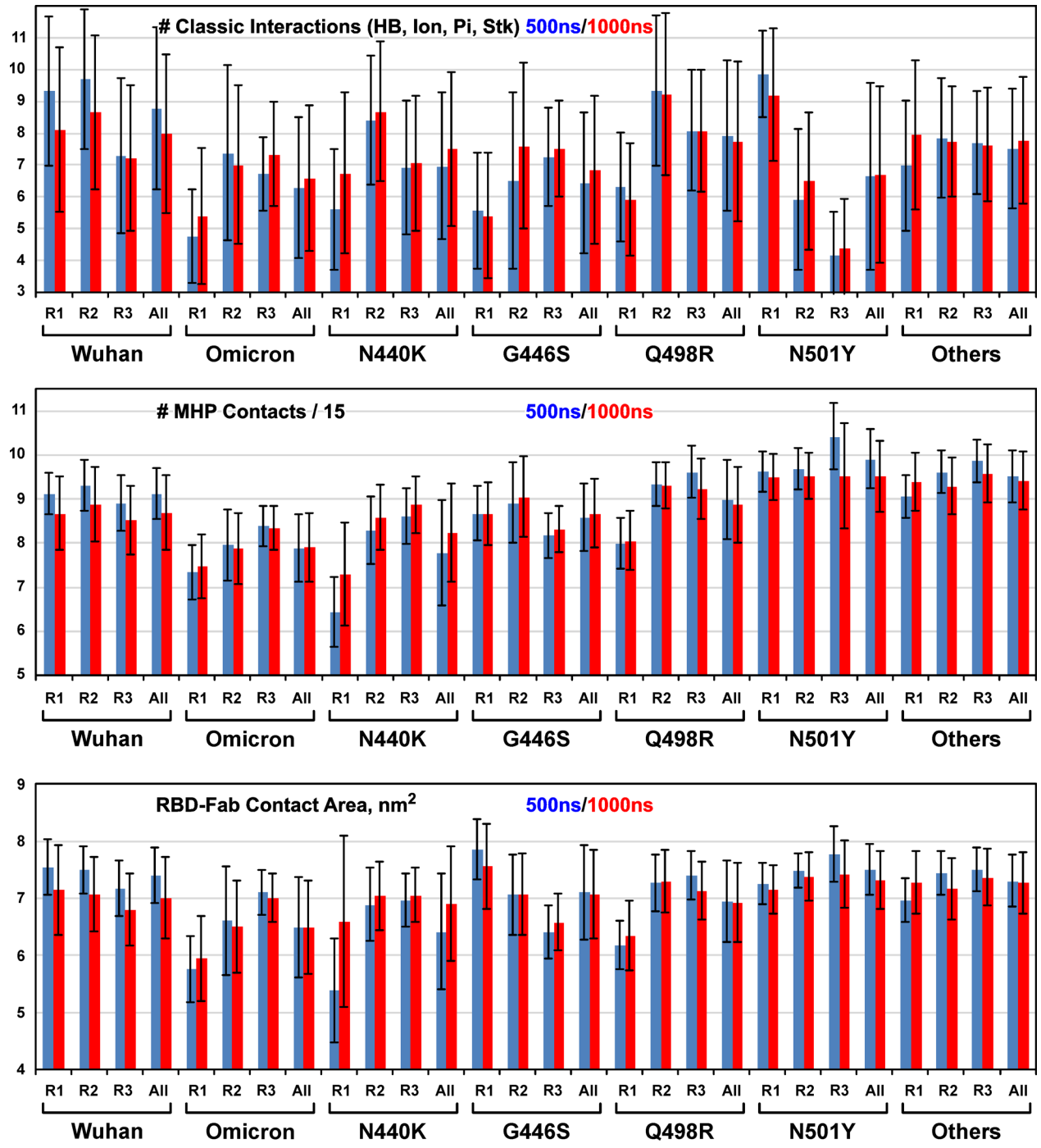

Supplementary Figure 10. Average characteristics of the 1-1000 ns and 500-1000 ns parts of the RBD/REGN10987-Fab MD trajectories (three replicas for each RBD variant, R1 to R3). Total number of 'classic' RBD-Fab interactions including ionic, hydrogen bonds, π-cation, and stacking contacts. Total number of molecular hydrophobicity potential (MHP) contacts includes hydrophobic-hydrophobic and polar-polar intermolecular interactions divided by 15. Data are presented as mean ± S.D. (n = T or 3*T, where T is the length of MD simulation in nanoseconds).

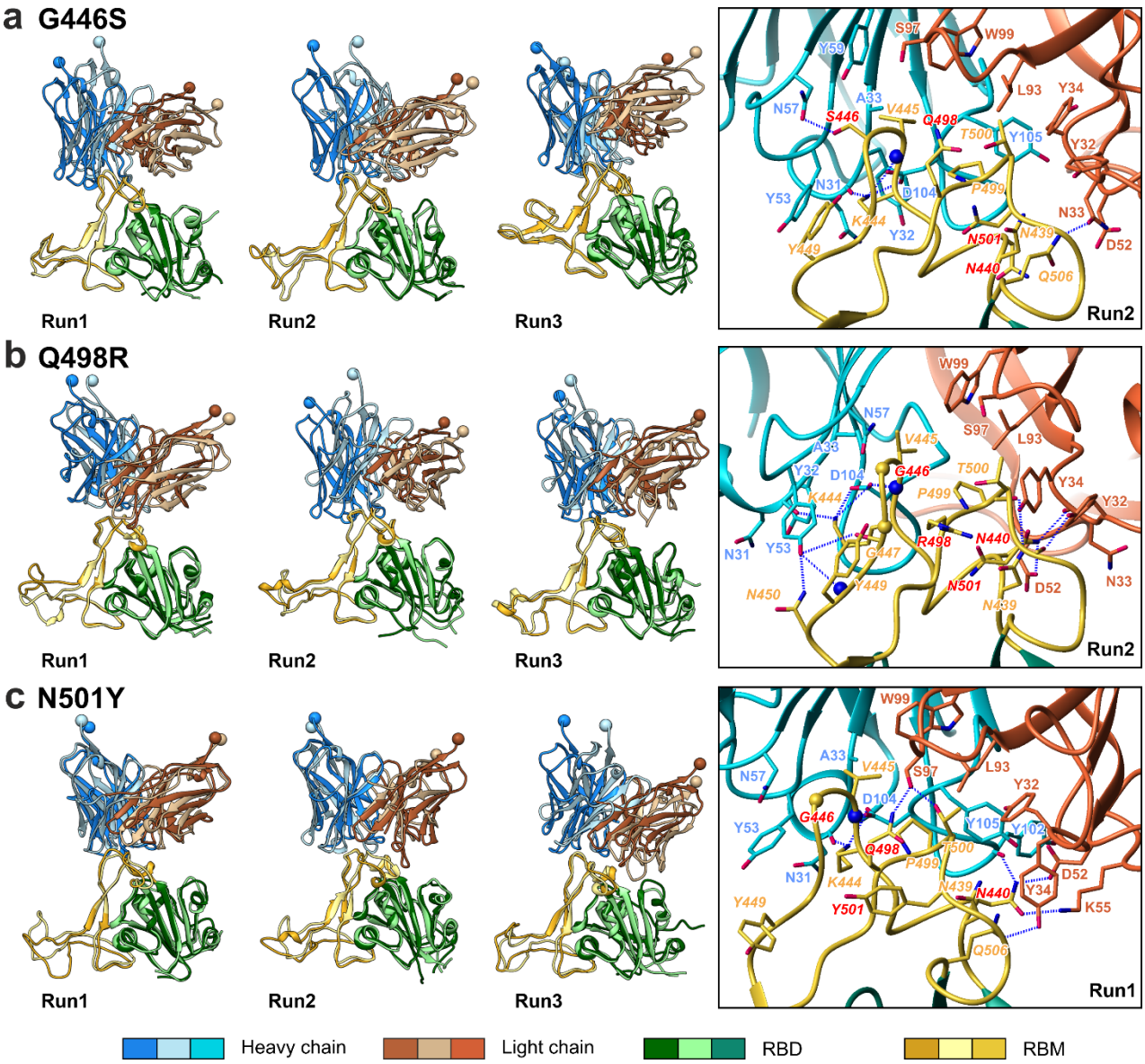

Supplementary Figure 11. Extreme (left panels) and mean (right panels, boxed) structures of the first eigenmode of motions from the 500-1000 ns part of 1 μs MD trajectories of the RBD/REGN10987-Fab complexes. The following RBD variants are shown: (a) Delta/G446S, (b) Delta/Q498R, (c) Delta/N501Y. Delta and Wuhan RBDs differ by two mutations (T478K and L452R). Residues of the RBD are in *italic* font. Residues mutated in the Omicron BA.1 variant are in red font. Hydrogen bonds are shown by dotted lines. CA atoms of Gly residues are shown by yellow spheres. Backbone NH atoms are shown by blue spheres. Backbone CO-groups are shown as sticks. On the left panels the RBD and *N*-terminal domain of Fab are shown for three MD replicas. To illustrate amplitude of motions, C' atoms of *C*-terminal residues of the Fab domain ($A121^{H}$ – heavy chain and $G111^{L}$ – light chain) are shown as spheres.

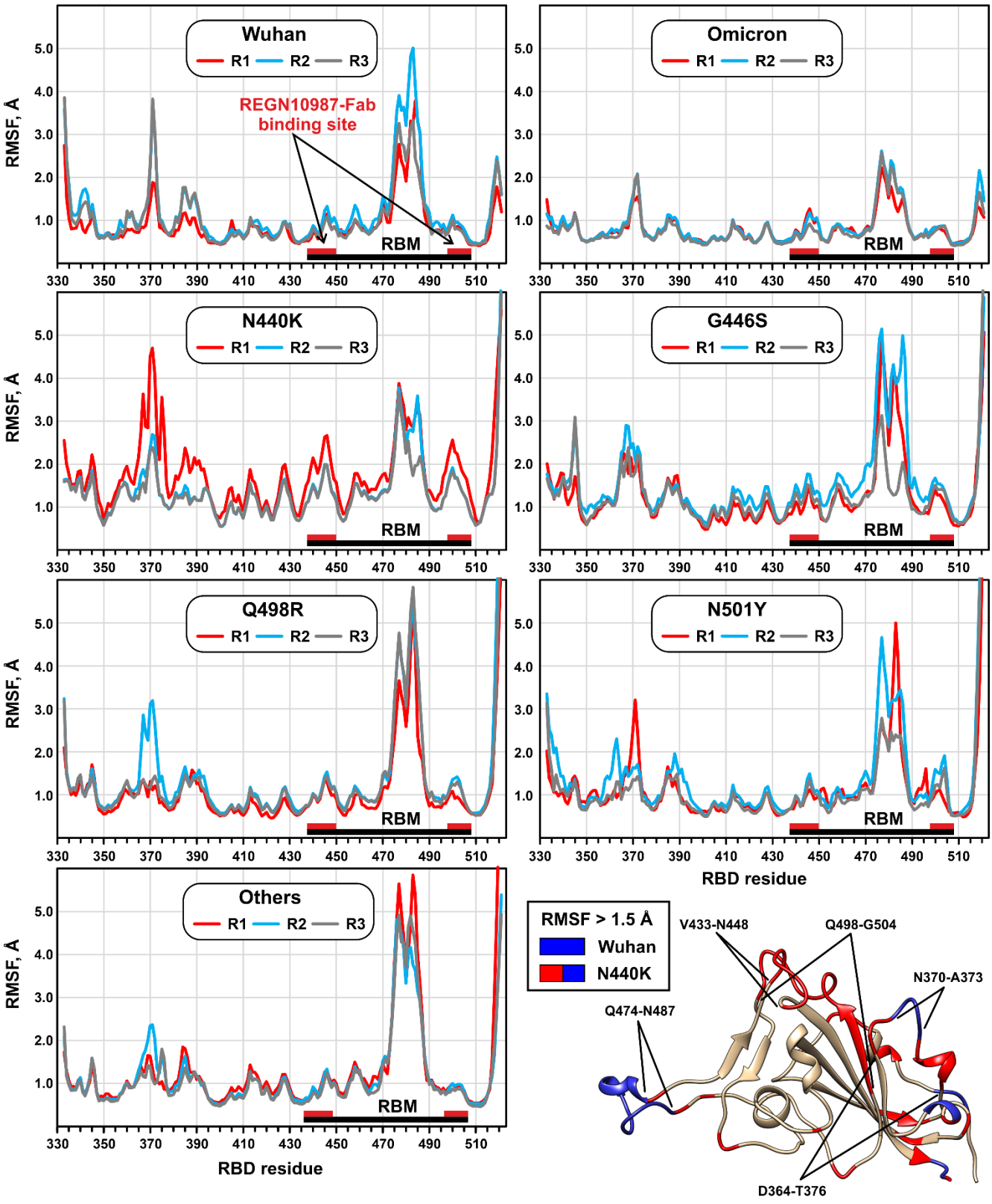

Supplementary Figure 12. Mobility of the RBDs in the complex with REGN10987-Fab. Root-mean-square fluctuation (RMSF) values in the 500-1000 ns parts of MD trajectories (three replicas for each RBD variant, R1 to R3) is shown in the upper left panels. (Right bottom panel) Backbone of the RBDs is colored according to the RMSF values in the MD trajectories of the Wuhan and N440K RBD variants. RMSF values were averaged over three replicas.

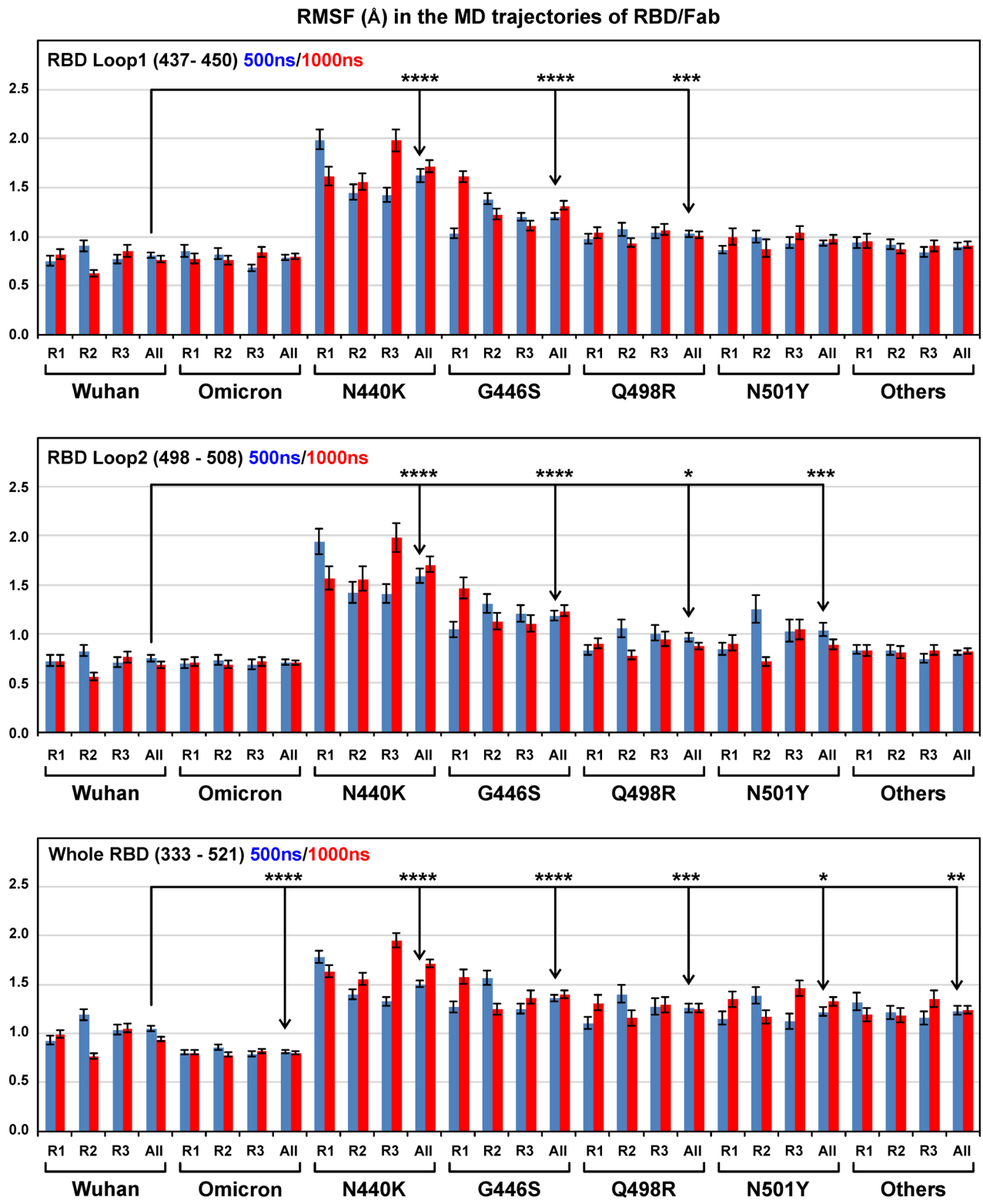

Supplementary Figure 13. Root-mean-square fluctuations (RMSFs) in the 1-1000 ns and 500-1000 ns parts of the RBD/REGN10987-Fab MD trajectories (three replicas for each RBD variant). Data are presented as mean ± S.E.M. (n = N or 3*N, where N is the number of residues in the fragment). *, **, ***, and **** ($p<0.05$, $p<0.01$, $p<0.001$, and $p<0.0001$) indicate significant differences from the Wuhan group according to one-way ANOVA/Dunnett test.

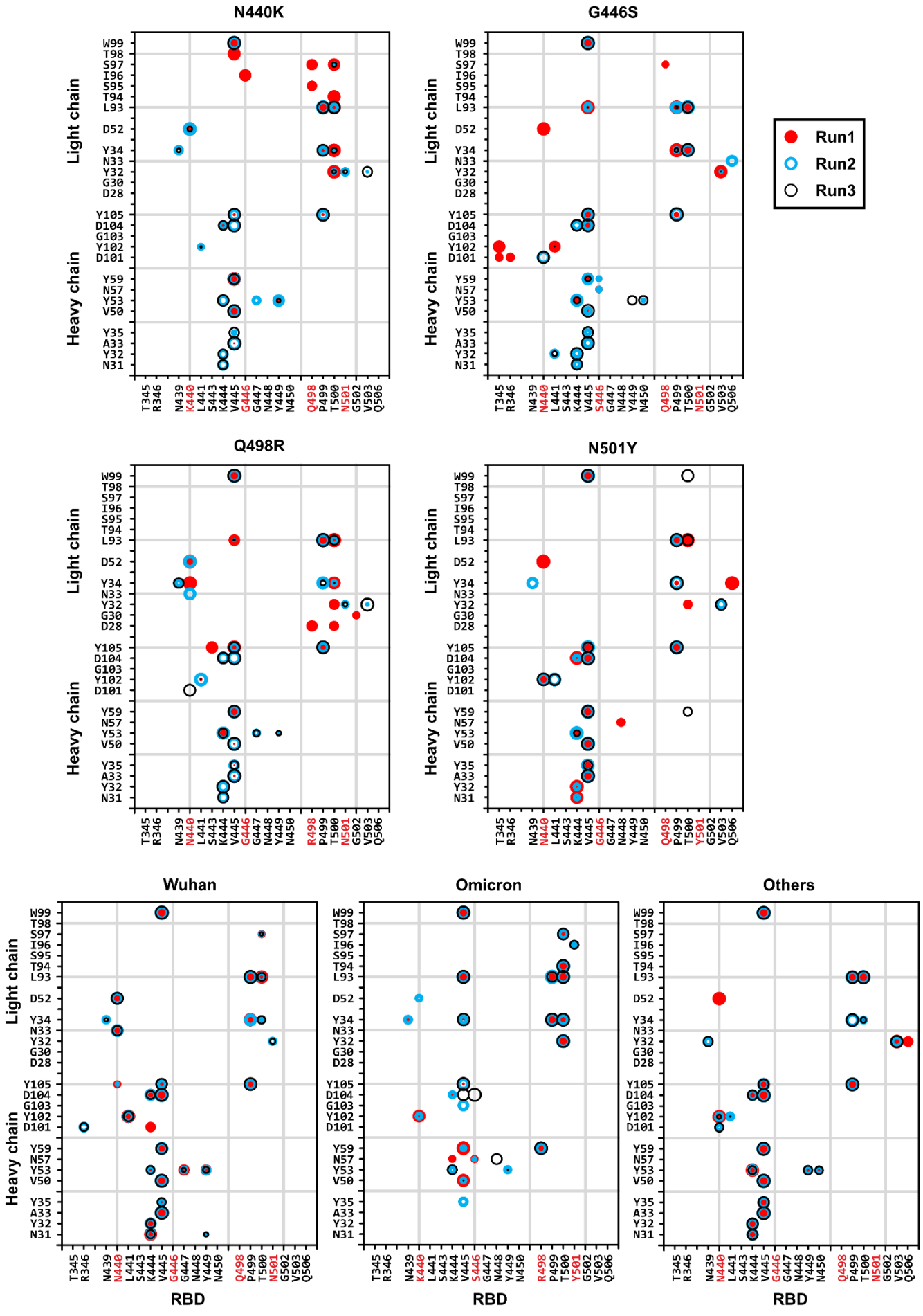
N440K
G446S
Q498R
N501Y
Wuhan
Omicron
Others
Light chain
Heavy chain
RBD
Run1
Run2
Run3

Supplementary Figure 14. Map of intermolecular interactions in the 500-1000 ns parts of the RBD/REGN10987-Fab MD trajectories (three replicas for each RBD variant). The interactions with lifetime greater or equal to 10 % of the MD replica length (500 ns) are shown as circles with the area proportional to the interaction lifetime. Color denotes different replicas (Run1, Run2, Run3).

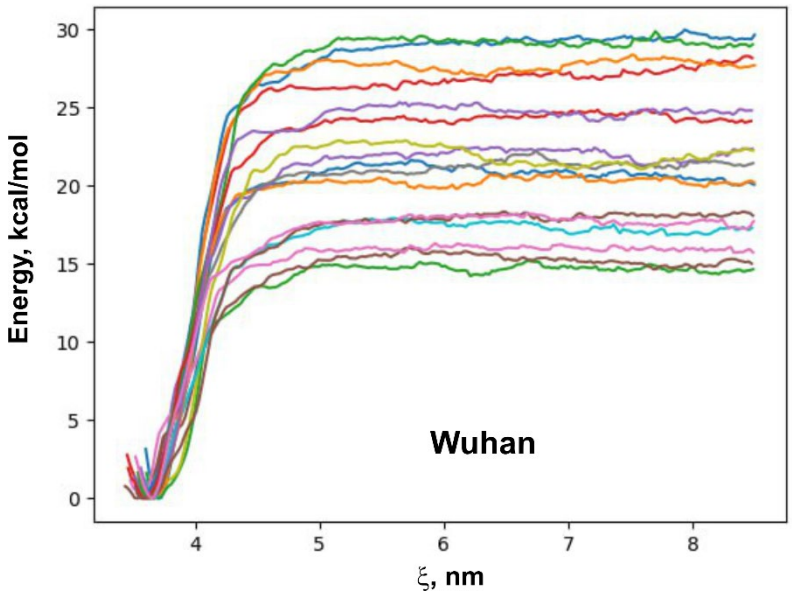

Supplementary Figure 15. Potential of mean force (PMF) profiles calculated for dissociation of the Wuhan RBD from the complex with *N*-terminal domain of REGN10987-Fab. 17 PMF profiles were calculated from the different starting points taken from three MD replicas. For each curve, the difference between the minimal and maximal values corresponds to the free energy of dissociation (ΔG^{calc}).

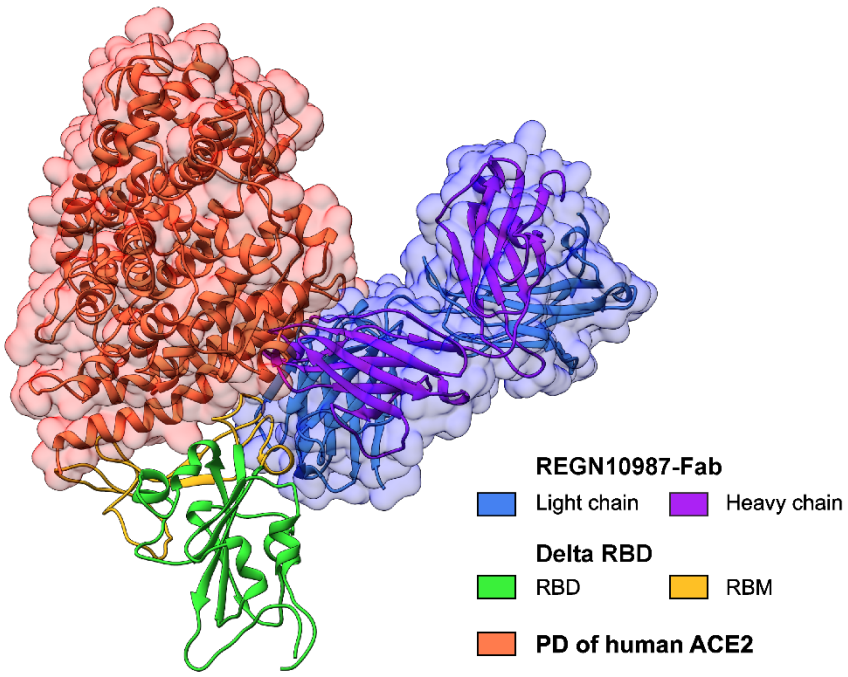

Supplementary Figure 16. The binding site of REGN10987-Fab partially overlaps with the ACE2 binding interface at the Delta RBD. Delta RBD/peptidase domain (PD) of human ACE2 complex is drawn according to 7W9C PDB [3].

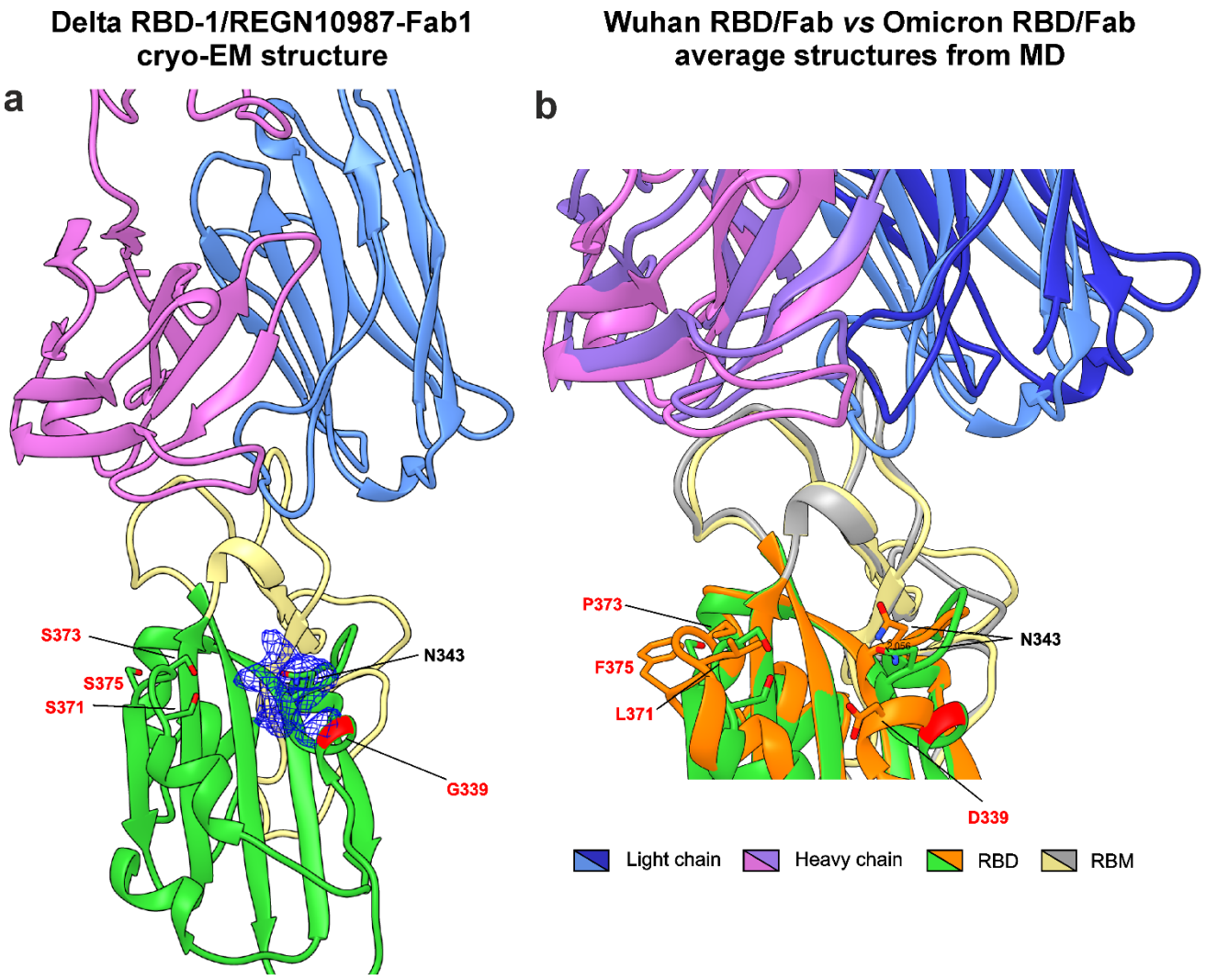

Supplementary Figure 17. Omicron mutations including G339D, S371L, S373P, and S375F affect the conformation of the T333-T345 and S366-S375 loops of the RBD and cause a displacement of the N343 glycan position by 2 Å towards the REGN10987-Fab binding site. (**a**) Cryo-EM structure of the RBD1/Fab1 fragment from the Delta S-protein/REGN10987-Fab structure. EM-density corresponding to N343 glycan is shown as blue mesh. (**b**) Superposition of the average structures from MD simulations of WT-RBD/Fab and Omicron-RBD/Fab. The displacement of the N343 sidechain is shown.

Supplementary references

[1] J. Hansen, A. Baum, K.E. Pascal, V. Russo, S. Giordano, E. Wloga, B.O. Fulton, Y. Yan, K. Koon, K. Patel, K.M. Chung, A. Hermann, E. Ullman, J. Cruz, A. Rafique, T. Huang, J. Fairhurst, C. Libertiny, M. Malbec, W.-Y. Lee, R. Welsh, G. Farr, S. Pennington, D. Deshpande, J. Cheng, A. Watty, P. Bouffard, R. Babb, N. Levenkova, C. Chen, B. Zhang, A. Romero Hernandez, K. Saotome, Y. Zhou, M. Franklin, S. Sivapalasingam, D.C. Lye, S. Weston, J. Logue, R. Haupt, M. Frieman, G. Chen, W. Olson, A.J. Murphy, N. Stahl, G.D. Yancopoulos, C.A. Kyratsous, Studies in humanized mice and convalescent humans yield a SARS-CoV-2 antibody cocktail, Science 369 (2020) 1010–1014. https://doi.org/10.1126/science.abd0827.

[2] J. Zhang, T. Xiao, Y. Cai, C.L. Lavine, H. Peng, H. Zhu, K. Anand, P. Tong, A. Gautam, M.L. Mayer, R.M. Walsh, S. Rits-Volloch, D.R. Wesemann, W. Yang, M.S. Seaman, J. Lu, B. Chen, Membrane fusion and immune evasion by the spike protein of SARS-CoV-2 Delta variant, Science 374 (2021) 1353–1360. https://doi.org/10.1126/science.abl9463.

[3] Y. Wang, C. Liu, C. Zhang, Y. Wang, Q. Hong, S. Xu, Z. Li, Y. Yang, Z. Huang, Y. Cong, Structural basis for SARS-CoV-2 Delta variant recognition of ACE2 receptor and broadly neutralizing antibodies, Nat. Commun. 13 (2022) 871. https://doi.org/10.1038/s41467-022-28528-w.